Thermodynamics and kinetics of cation ordering in natural and synthetic Mg(Al,Fe^{3+})$_2$O$_4$ spinels from in situ high-temperature X-ray diffraction

F. Martignago,[1] G.B. Andreozzi,[2] and A. Dal Negro[1,*]

[1]Dipartimento di Mineralogia e Petrologia, University of Padova, Corso Garibaldi 37, I-35137, Italy
[2]Dipartimento di Scienze della Terra, University of Roma "La Sapienza", P.le A. Moro 5, I-00185, Italy

Abstract

One natural and two synthetic spinels with compositions Mg(Al$_{1-z}$Fe$_z^{3+}$)$_2$O$_4$ (with $2z = 0.078, 0.138$, and 0.200, respectively) were studied by in situ, high-temperature, single-crystal X-ray diffraction. All samples were heated from room temperature to 1050 °C. Thermal expansion was monitored by measuring the cell edge variation. Cation disorder was monitored by measuring the variation of the oxygen positional parameter u, which is closely correlated with the inversion parameter i. All samples showed extensive Al reordering at the M site between 550 and 650 °C, followed by an increase of disorder at $T > 650$ °C due to both Mg-Al and Mg-Fe^{3+} intersite exchanges.

The measured cation distributions were compared with those calculated using the general thermodynamic model for spinel binary solid-solutions of O'Neill and Navrotsky (1984). Measured and calculated inversion parameters compare satisfactorily at $T > 650$ °C, i.e., at conditions under which equilibrium was achieved at any temperature. In fact, at $T > 650$ °C, both ^{IV}Fe^{3+} and ^{IV}Al increase with increasing T, following the equilibrium path. The reproducibility of ^{IV}Al occupancies was very high, whereas ^{IV}Fe^{3+} occupancies were not satisfactorily matched. The cation distribution relaxation observed between 550 and 650 °C was interpreted on the basis of kinetic considerations. In this temperature range, inversion decreases to a minimum because the amounts of Al that reorder are far more abundant than those of Fe^{3+} that disorder. The Mg-Fe^{3+} exchange was confirmed to proceed at a faster rate than the Mg-Al exchange. Moreover, the Mg-Fe^{3+} exchange was found to be active at laboratory times at about 550 °C, whereas the Mg-Al exchange was hard to monitor below 600 °C.

Keywords: X-ray diffraction, in situ-HT, order-disorder, spinels

Introduction

Spinel-group minerals are characterized by a non-convergent, temperature-dependent cation order/disorder, i.e., no change of symmetry is associated with cation disordering. Cation distribution can be described by the ^{IV}(A$_{1-i}$B$_i$)^{VI}(B$_{2-i}$A$_i$)O$_4$ structural formula, where IV and VI represent the tetrahedrally and octahedrally coordinated T and M sites, respectively, A and B are cations with different valences, and i represents the inversion parameter. At low temperature, i tends to 0 in normal spinels [e.g., spinel s.s. ^{IV}(Mg)^{VI}(Al)$_2$O$_4$] and to 1 in inverse spinels [e.g., magnesioferrite ^{IV}(Fe^{3+})^{VI}(MgFe^{3+})O$_4$], which are both ordered. At high temperature, cation disorder increases and i values have been shown to converge asymptotically toward 2/3 for all compositions (Harrison et al. 1998; O'Neill et al. 1992; O'Neill and Dollase 1994; Redfern et al. 1999; Andreozzi et al. 2000; Carbonin et al. 2002; Martignago et al. 2003).

The influence of non-Al cations on the Mg-Al order-disorder reaction has been recently studied by Martignago et al. (2003) using a natural, highly ordered, Fe^{3+}-bearing spinel. Their results indicate that the Fe^{3+} cation triggers trivalent-divalent cation exchange at $T \geq 550$ °C. This agrees with the results obtained by

Andreozzi et al. (2001) for the synthetic spinel-magnesioferrite series, which showed that Fe^{3+} partitions between the M and T sites as a function of both magnesioferrite component and temperature. Moreover, Martignago et al. (2003) observed that at the lowest temperatures order-disorder is controlled by a two-stage kinetic process, with a rapid intersite exchange of Fe^{3+} with Mg followed by a slow exchange of Mg with Al.

Andreozzi and Princivalle (2002) quantitatively described the kinetics of Mg-Al exchange in MgAl$_2$O$_4$ spinel using the Mueller (1967, 1969) model. Following O'Neill (1994), these authors described the order-disorder process with the chemical exchange reaction ^{IV}Al + ^{VI}Mg = ^{IV}Mg + ^{VI}Al, the forward reaction accounting for the exchange of Al at the T site with Mg at the M site (ordering), and the backward reaction for the exchange of Mg at the T site with Al at the M site (disordering). These homogeneous reactions were assumed to be second-order chemical reactions, and first-order with respect to the concentration at one site (Ganguly 1982). The time rate of change of concentration of Al at the T site ($= i$), was expressed as $-\mathrm{d}i/\mathrm{d}t = K[i^2 - K_D(1-i)(2-i)]$, where K_D, the equilibrium constant of the exchange reaction, is a function of temperature and pressure alone. The variation of i with time was revealed to only depend on the initial and final inversion degrees, and on the rate constant K. The kinetics of Mg-Fe^{3+} exchange in MgFe$_2$O$_4$ spinel was

expressed by O'Neill (1994) in terms of the Mueller rate law and by Harrison and Putnis (1999) in terms of the Ginzburg-Landau rate law. The Mueller rate law is a special case of the more general Ginzburg-Landau rate law, but it only applies to homogeneous ordering. However, the Ginzburg-Landau rate law is rather complex and cannot easily be applied to the routine quantification of macroscopic observations. To this purpose, the Mueller rate law or the Ginzburg-Landau rate law for homogeneous ordering are more functional. Accordingly, Harrison and Putnis (1999) fitted the data of O'Neill (1994) by combining the Ginzburg-Landau rate law with the standard Landau potential for a homogeneous crystal, although they had described the kinetics of Mg-Fe^{3+} at a microscopic scale with a heterogeneous mechanism.

In the present study, one natural and two synthetic Fe^{3+}-bearing spinels were studied by in situ, high-temperature, single-crystal X-ray diffraction. The selected specimens were (1) two synthetic crystals with composition $Mg(Fe^{3+}_zAl_{1-z})_2O_4$, with $2z$ of 0.138 (MgF14) and 0.200 (MgF20) atoms per formula unit (apfu), which had been previously analyzed by electron microprobe analysis and Mössbauer spectroscopy by Andreozzi et al. (2001), and (2) a natural, green, ferrian variety of spinel solid solution (obsolete mineral name: chlorospinel) with composition $Mg(Fe^{3+}_zAl_{1-z})_2O_4$ with $2z$ of 0.078 apfu (3dis), from a magnetite-bearing chlorite schist from the Shishimsk Mountains, Urals, Russia (Bothwell and Hey 1958). The natural spinel shows a much higher degree of cation order, due to cooling on a geological time scale, than do the quenched synthetic ones. To achieve a comparable initial configuration, the natural spinel sample 3dis was equilibrated at 1000 °C for 24 hours and then quenched before subsequent in situ measurements. On the basis of the oxygen positional parameter (*u*) measured at room temperature the equilibrium temperature after quenching was estimated to be about 800 °C. This value is comparable with those estimated by Andreozzi et al. (2001) for the synthetic samples MgF14 and MgF20.

The aim of this work is to compare natural and synthetic spinels with respect to (1) the evolution of structural state with temperature, and (2) the influence of Fe^{3+} content on the disordering pathway. The *u* parameter was chosen to monitor the evolution of the spinel structural state as it can be measured routinely with both extreme accuracy and precision. Cation distribution at each temperature was obtained using the bond-length model, applying thermal expansion to pure bond lengths (Carbonin et al. 2002).

EXPERIMENTAL METHODS

Data collection

X-ray diffraction data were collected up to $2\theta = 75°$ (Mo$K\alpha$ radiation monochromatized by a flat graphite crystal) due to obstacles in the circle movements with the microfurnace (Carbonin et al. 2002) using a Siemens Aed II 4-circle single-crystal diffractometer. Intensity data were measured for the same set of 87 independent reflections for each crystal for all heating experiments, using the ω-2θ scan mode, with profile recording of each reflection. The data were collected at temperatures ranging from room temperature to 1050 °C in a controlled atmosphere (N_2) using a microfurnace installed on the diffractometer (Molin et al. 2001; Carbonin et al. 2002). For most experiments the collection time was about 2 h, including the time required for orientation-matrix and cell-parameter measurement (50 min). At 700 °C, the three crystals were maintained at the same temperature for about 15 hours before data collection, to approach equilibrium as closely as possible (cf. Andreozzi and Princivalle 2002). As done in previous studies (Carbonin et al. 2002; Martignago et al. 2003), several back-and-forth experiments were carried out from room temperature up to 500 °C, continuously monitoring the oxygen

coordinate *u*, which is order-dependent at a given temperature. It was noted that in this temperature range the coordinate remained constant.

For all heating experiments, intensities were corrected for spherical absorption by taking into account the mean radius of the crystal. The unit-cell parameter (*a*) was determined at each temperature by centering 24 reflections in the range $25° < \theta < 34°$. Each reflection was centered at both positive and negative values of 2θ and ω angles using the step-scan routine. The mean of the ω centers was taken as the true value.

Structural refinements

Structural refinements were carried out with the Shelxl-97 program (Sheldrick 1997) in the $Fd\overline{3}m$ space group (with origin at $\overline{3}m$) without chemical constraints. No violations of this symmetry were detected. Scale factor, secondary extinction coefficient, oxygen positional parameter *u*, anisotropic displacement parameters $U(O)$, $U(M)$, and $U(T)$, and site mean atomic numbers (m.a.n.) were considered as variables. For samples MgF14 and 3dis, the scattering curves of Mg^{2+} and $Al^{1.5+}$, not constrained to full site occupancy because of the Mg-Al inversion, were assigned to the T and M sites, respectively. For sample MgF20, the scattering curve for Mg^{2+} was assigned to the T sites and the scattering curves of Al^{3+} and Fe^{3+} were assigned to M sites. It is well known that in spinels the site m.a.n. are sensitive to the ionization level of oxygen (Della Giusta et al. 1986). Following the procedure described in Salviulo et al. (2000), the ionization level for the O-scattering curve was allowed to vary between $O^{1.5-}$ and O^{2-}, and refined so as to obtain the best conventional agreement factors and total m.a.n. corresponding to those expected from stoichiometry ($\pm 1\sigma$).

The results of the structural refinements are given in Table 1.

Sample characterization and cation distribution

After data collection, chemical analyses were performed on the polished surface of the same single crystals used for X-ray study, using the Cameca/Camebax Microbeam electron microprobe at the Istituto di Geoscienze e Georisorse, CNR Padova. Analyses were performed at 15 kV and 15 nA sample current using the wavelength dispersive method (WDS). X-ray counts were converted into oxide weight percentages using the PAP correction program supplied by CAMECA. A synthetic spinel ($MgAl_2O_4$) and synthetic oxides were used as standards. The results of the microprobe analysis are reported in Table 2.

At room temperature, the inversion parameter i [$= {}^{IV}(Al + Fe^{3+})$] was obtained according to the bond-length method, following Carbonin et al. (1996) and using ionic radii from Lavina et al. (2002). This method determines cation distributions by minimizing the following function, which takes into account structural data, using a soft chemical constraint:

$$F(X_i) = 1/n \sum_{1}^{n} {}_j \{[O_j - C_j(X_i)]/\sigma_j\}^2 \qquad (1)$$

O_j are the observed quantities with their standard deviation σ_j. In particular, O_j are the four observed crystallographic parameters (*a*, *u*, and m.a.n. of T and M sites) and the chemical atomic proportions (at least two) for a total of *n*. $C_j(X_i)$ are the corresponding quantities calculated by means of variable cation fractions X_i. $F(X_i)$ values $\cong 1$ mean good agreement among calculated and observed data. Since the values of the atomic fractions are strongly correlated by crystal chemical constraints, evaluation of their standard deviation is not easy. Nevertheless, the reliability of the resulting distribution can be tested by scanning $F(X_i)$ at fixed values of each atomic fraction X_i in a range around the minimum. The variation of each atomic fraction that leads to doubling of the minimized $F(X_i)$ may be assumed as the uncertainty of its optimized value. Table 3 reports the $F(X_i)$ values.

At all temperatures except room *T*, the *i* parameter was determined by applying the thermal expansion coefficient α_1 (see next section) to pure bond lengths (Carbonin et al. 2002; Martignago et al. 2003).

RESULTS AND DISCUSSION

The variation of the cell edge with *T* is not linear in the investigated temperature range, but can be approximated by two distinct regression lines of the type $a = a_0 (1 + \alpha\Delta T)$, with different values for α at low (α_1) and high (α_2) temperatures (Fig. 1). The thermal expansion coefficient α_1, which refers to the pure thermal expansion, is slightly lower than α_2, which also depends on cation exchange. The greatest differences between the α_1 and α_2 coefficients are shown by the 3dis sample in which the cation

TABLE 1. Structure refinement results

Sample	T (°C)	a (Å)	u	M-O (Å)	T-O (Å)	$M_{m.a.n.}$	$T_{m.a.n.}$	$Tot_{m.a.n.}$	$U_{eq}(O)$ (Å²)	$U_{eq}(M)$ (Å²)	$U_{eq}(T)$ (Å²)	R_{all}%	wR_2%
MgF20	25	8.1154(3)	0.26180(7)	1.938(1)	1.923(1)	13.66(61)	13.49(9)	40.80(1.23)	0.0081(2)	0.0060(2)	0.0041(3)	1.88	3.66
	200	8.1256(2)	0.26177(8)	1.940(1)	1.925(1)	13.66(65)	13.55(9)	40.86(1.30)	0.0098(3)	0.0076(2)	0.0063(3)	1.95	4.02
	400	8.1399(4)	0.26177(8)	1.944(1)	1.928(1)	13.60(61)	13.46(8)	40.66(1.23)	0.0127(2)	0.0102(2)	0.0088(3)	1.89	3.67
	450	8.1438(4)	0.26176(8)	1.945(1)	1.929(1)	13.57(59)	13.44(8)	40.80(1.17)	0.0134(2)	0.0106(2)	0.0091(3)	1.80	3.45
	500	8.1482(3)	0.26171(8)	1.946(1)	1.929(1)	13.62(62)	13.42(8)	40.66(1.24)	0.0141(3)	0.0113(2)	0.0101(3)	1.82	3.67
	550	8.1520(5)	0.26179(8)	1.947(1)	1.931(1)	13.69(62)	13.49(8)	40.87(1.24)	0.0145(3)	0.0119(2)	0.0107(3)	1.91	3.69
	600	8.1564(5)	0.26173(8)	1.948(1)	1.932(1)	13.50(60)	13.29(8)	40.30(1.20)	0.0156(3)	0.0125(2)	0.0115(3)	2.01	3.61
	650	8.1606(5)	0.26179(9)	1.949(1)	1.933(1)	13.80(50)	13.32(10)	40.93(1.40)	0.0155(3)	0.0124(2)	0.0118(3)	2.12	4.77
	700	8.1643(5)	0.26161(8)	1.951(1)	1.932(1)	13.67(59)	13.53(8)	40.87(1.18)	0.0167(3)	0.0140(2)	0.0131(3)	2.02	3.42
	800	8.1721(6)	0.26143(9)	1.954(1)	1.931(1)	13.71(68)	13.48(9)	40.90(1.35)	0.0189(3)	0.0158(2)	0.0145(3)	2.48	3.94
	900	8.1800(7)	0.26117(11)	1.958(1)	1.929(2)	13.60(78)	13.48(10)	40.69(1.57)	0.0202(4)	0.0169(3)	0.0158(4)	2.30	4.32
	1000	8.1871(7)	0.26110(9)	1.960(1)	1.930(1)	13.61(63)	13.63(8)	40.86(1.26)	0.0218(3)	0.0182(2)	0.0177(3)	2.28	3.52
	1050	8.1898(7)	0.26102(10)	1.961(1)	1.929(1)	13.43(66)	13.45(8)	40.31(1.33)	0.0230(3)	0.0187(2)	0.0180(4)	2.53	3.80
MgF14	25	8.1082(6)	0.26174(10)	1.936(1)	1.920(1)	13.58(5)	13.24(10)	40.40(14)	0.0072(3)	0.0041(2)	0.0033(3)	2.14	4.15
	200	8.1184(6)	0.26177(9)	1.939(1)	1.923(1)	13.61(5)	13.38(9)	40.59(13)	0.0088(2)	0.0058(2)	0.0055(3)	2.01	3.51
	400	8.1328(5)	0.26178(10)	1.942(1)	1.927(1)	13.68(5)	13.50(10)	40.85(14)	0.0109(3)	0.0080(2)	0.0082(3)	2.32	3.93
	450	8.1365(7)	0.26176(10)	1.943(1)	1.927(1)	13.59(5)	13.35(10)	40.54(14)	0.0119(3)	0.0084(2)	0.0085(3)	2.37	4.19
	500	8.1408(7)	0.26174(11)	1.944(1)	1.928(2)	13.64(5)	13.38(10)	40.66(15)	0.0126(3)	0.0093(3)	0.0093(4)	2.64	4.35
	550	8.1447(5)	0.26178(11)	1.945(1)	1.929(2)	13.56(5)	13.33(10)	40.46(15)	0.0136(3)	0.0099(3)	0.0101(4)	2.45	4.56
	600	8.1489(7)	0.26173(11)	1.946(1)	1.930(2)	13.60(5)	13.39(10)	40.60(15)	0.0139(3)	0.0104(2)	0.0109(4)	2.92	4.49
	650	8.1529(7)	0.26198(11)	1.946(1)	1.934(2)	13.62(5)	13.40(10)	40.63(14)	0.0145(3)	0.0111(3)	0.0116(4)	2.48	4.10
	700	8.1571(9)	0.26179(11)	1.948(1)	1.933(2)	13.54(5)	13.31(10)	40.38(15)	0.0161(3)	0.0119(3)	0.0125(4)	3.01	4.42
	800	8.1648(9)	0.26158(13)	1.951(1)	1.931(2)	13.45(6)	13.26(12)	40.16(16)	0.0178(4)	0.0132(3)	0.0137(4)	2.95	5.16
	900	8.1727(9)	0.26136(14)	1.955(1)	1.930(2)	13.53(6)	13.27(12)	40.34(17)	0.0192(4)	0.0147(3)	0.0151(5)	3.19	5.52
	1000	8.1802(9)	0.26118(16)	1.958(1)	1.929(2)	13.44(7)	13.22(14)	40.11(20)	0.0213(5)	0.0163(4)	0.0167(5)	3.47	6.50
	1050	8.1841(9)	0.26098(15)	1.960(1)	1.928(2)	13.40(7)	13.21(13)	40.02(19)	0.0218(5)	0.0168(3)	0.0168(5)	3.61	5.74
3dis	25*	8.0973(5)	0.26323(6)	1.923(1)	1.939(1)	13.58(4)	12.62(7)	39.78(10)	0.0042(2)	0.0037(2)	0.0041(2)	1.48	3.05
	25†	8.0937(5)	0.26167(7)	1.934(1)	1.916(1)	13.28(4)	12.98(7)	39.53(10)	0.0081(2)	0.0048(2)	0.0042(2)	1.46	2.93
	200	8.1039(3)	0.26173(8)	1.936(1)	1.919(1)	13.22(5)	12.89(8)	39.32(12)	0.0100(2)	0.0066(2)	0.0062(2)	1.78	3.56
	400	8.1179(6)	0.26154(9)	1.940(1)	1.920(1)	13.30(5)	12.89(9)	39.49(13)	0.0123(3)	0.0090(2)	0.0084(3)	1.91	4.19
	450	8.1219(6)	0.26159(9)	1.941(1)	1.921(1)	13.31(5)	12.89(9)	39.51(14)	0.0130(3)	0.0098(2)	0.0093(3)	1.65	3.75
	500	8.1256(7)	0.26158(9)	1.942(1)	1.922(1)	13.34(5)	12.89(9)	39.58(13)	0.0134(3)	0.0105(2)	0.0098(3)	1.77	3.69
	550	8.1292(6)	0.26160(8)	1.943(1)	1.923(1)	13.23(5)	12.83(8)	39.30(13)	0.0143(3)	0.0109(2)	0.0104(3)	1.96	3.72
	600	8.1340(7)	0.26206(6)	1.940(1)	1.931(1)	13.16(3)	12.79(6)	39.12(8)	0.0146(2)	0.0112(2)	0.0121(2)	1.62	2.64
	650	8.1386(8)	0.26206(8)	1.941(1)	1.932(1)	13.24(4)	12.85(7)	39.32(11)	0.0149(2)	0.0117(2)	0.0123(3)	1.91	3.38
	700	8.1423(8)	0.26189(8)	1.944(1)	1.930(1)	13.17(4)	12.84(8)	39.19(12)	0.0162(3)	0.0125(2)	0.0130(3)	2.16	3.56
	800	8.1500(8)	0.26166(9)	1.947(1)	1.929(1)	13.13(5)	12.83(9)	39.09(13)	0.0182(3)	0.0137(2)	0.0143(3)	2.13	3.94
	900	8.1581(7)	0.26136(9)	1.951(1)	1.927(1)	13.24(5)	12.98(8)	39.46(13)	0.0195(3)	0.0156(2)	0.0160(3)	2.68	3.72
	1000	8.1652(8)	0.26110(9)	1.955(1)	1.925(1)	13.19(4)	12.94(8)	39.32(11)	0.0215(3)	0.0171(2)	0.0175(3)	2.39	3.58
	1050	8.1678(8)	0.26107(10)	1.956(1)	1.925(1)	13.15(5)	12.98(8)	39.29(12)	0.0224(3)	0.0177(3)	0.0179(4)	2.69	3.86

Notes: Estimated standard deviation in brackets; R_{all} and wR_2 = agreement factors from the SHELXL-97 program package.
* Untreated sample.
† Sample quenched from 1000 °C.

exchange begins at a lower temperature with respect to the synthetic samples. Their best-fit values are reported in Table 4.

The oxygen positional parameter u is strongly influenced by intersite cation exchange and, conversely, it is closely correlated with the T-dependent inversion parameter i. As observed by Carbonin et al. (2002) and Martignago et al. (2003), u remained constant and thermal expansion was completely reversible until the onset of cation exchange.

For sample MgF20, the variations of u as a function of temperature are shown in Figure 2a. At room temperature, the u value is 0.26180 and this remains constant (within 1σ) up to 650 °C. At higher temperature, the crystal begins to disorder and u continuously decreases, reaching a value of 0.26102 at 1050 °C.

In sample MgF14 (Fig. 2b), u remains almost constant at 0.2617 up to 600 °C, suddenly increases to 0.26198 at T = 650 °C, and then continuously decreases to 0.26098, a value similar to that reached by sample MgF20.

In sample 3dis, the value of u measured at room temperature from the untreated crystal (0.26323) is much higher than those observed from the MgF20 and MgF14 samples (Fig. 2c), and corresponds to an inversion value of 0.14. After annealing at 1000 °C for 24 hours followed by quenching, the u value becomes

TABLE 2. Chemical composition by electron microprobe

Sample	MgF20	MgF14	3dis
MgO	27.08 (12)	27.97(40)	27.27(17)
Al$_2$O$_3$	61.71 (24)	64.26 (12)	66.69 (17)
MnO	–	–	0.11 (3)
ZnO	–	–	0.23 (3)
FeO	10.71(31)	7.55(17)	4.23 (29)
Σ	99.5	99.78	98.53
Cations on basis of four oxygen atoms per formula unit			
Mg	0.999 (10)	1.016 (10)	0.994 (10)
Al	1.800 (10)	1.846 (10)	1.922 (10)
Mn	–	–	0.002 (1)
Zn	–	–	0.004 (1)
Fe^{3+}	0.200(10)	0.138 (10)	0.078 (10)
Σ	2.999	3.000	3.000

Notes: Average of 30 analyses; estimated standard deviation in brackets.

0.26167, i.e., similar to those measured at room temperature for the synthetic samples and comparable with that of sample 3dis heated to 800 °C. During heating experiments, the u value remains almost constant up to 550 °C, suddenly increases to 0.26206 at 600 °C, and then decreases continuously from 650 to 1050 °C, as observed for sample MgF14.

Andreozzi et al. (2001) calculated a temperature of apparent equilibration of about 800 °C for the two synthetic samples

TABLE 3. Cation distribution between the T and M sites as a function of temperature

Sample	T (°C)	T site			M site			i*	$F(X_i)$
		Al	Fe^{3+}	Mg	Al	Fe^{3+}	Mg		
MgF20									
	25	0.182	0.093	0.726	1.617	0.108	0.274	0.27	0.20
	200	0.183	0.098	0.719	1.619	0.101	0.279	0.28	0.81
	400	0.187	0.091	0.721	1.614	0.108	0.278	0.28	0.93
	450	0.186	0.090	0.724	1.615	0.110	0.275	0.28	0.83
	500	0.190	0.088	0.722	1.610	0.112	0.277	0.28	0.47
	550	0.182	0.093	0.725	1.619	0.106	0.274	0.28	0.47
	600	0.193	0.079	0.729	1.608	0.121	0.271	0.27	0.37
	650	0.187	0.081	0.732	1.614	0.119	0.267	0.27	0.34
	700	0.197	0.094	0.710	1.601	0.107	0.292	0.29	0.14
	800	0.212	0.089	0.700	1.586	0.112	0.302	0.30	1.77
	900	0.229	0.087	0.685	1.568	0.115	0.317	0.32	1.77
	1000	0.229	0.098	0.673	1.568	0.103	0.329	0.33	0.40
	1050	0.244	0.084	0.672	1.553	0.117	0.330	0.33	1.70
MgF14									
	25	0.207	0.061	0.731	1.638	0.079	0.283	0.27	0.45
	200	0.205	0.062	0.732	1.639	0.081	0.280	0.27	0.84
	400	0.206	0.065	0.728	1.638	0.077	0.284	0.27	0.89
	450	0.207	0.058	0.734	1.637	0.084	0.279	0.27	0.88
	500	0.210	0.059	0.731	1.635	0.083	0.282	0.27	0.83
	550	0.206	0.060	0.734	1.639	0.082	0.278	0.27	0.62
	600	0.209	0.059	0.731	1.634	0.083	0.282	0.27	0.55
	650	0.190	0.060	0.750	1.654	0.083	0.263	0.25	0.72
	700	0.204	0.060	0.736	1.641	0.081	0.278	0.26	0.45
	800	0.220	0.062	0.717	1.624	0.078	0.298	0.28	0.44
	900	0.237	0.056	0.708	1.607	0.085	0.308	0.29	0.55
	1000	0.248	0.059	0.693	1.596	0.081	0.323	0.31	0.61
	1050	0.262	0.060	0.678	1.581	0.080	0.339	0.32	0.85
3dis									
	25*	0.126	0.015	0.847	1.788	0.067	0.143	0.14	0.85
	25†	0.239	0.036	0.718	1.679	0.049	0.272	0.28	0.87
	200	0.239	0.033	0.720	1.690	0.040	0.268	0.27	1.49
	400	0.254	0.028	0.710	1.670	0.051	0.279	0.28	1.39
	450	0.251	0.028	0.714	1.673	0.051	0.275	0.28	1.29
	500	0.252	0.026	0.715	1.671	0.054	0.274	0.28	1.26
	550	0.250	0.029	0.714	1.679	0.045	0.276	0.28	1.17
	600	0.215	0.033	0.745	1.713	0.041	0.246	0.25	1.07
	650	0.214	0.033	0.746	1.709	0.045	0.245	0.25	0.81
	700	0.223	0.034	0.736	1.701	0.043	0.256	0.26	0.66
	800	0.241	0.035	0.717	1.685	0.040	0.275	0.28	0.82
	900	0.262	0.037	0.694	1.652	0.049	0.299	0.30	0.35
	1000	0.284	0.035	0.675	1.633	0.049	0.319	0.32	0.16
	1050	0.283	0.040	0.671	1.631	0.045	0.324	0.32	0.30

Notes: *i = inversion degree (Al + Fe^{3+} at the T site); $F(X_i)$ sum of square residuals, (Eq. 1); Estimated uncertainties for Fe^{3+}, Al, and Mg are 0.005, 0.017, and 0.018, respectively.
* Untreated sample.
† Sample quenched from 1000 °C.

TABLE 4. Best fit values of thermal expansion coefficient

Sample	T range (°C)	a (Å)	$\alpha_1 \times 10^{-6}$ (°C^{-1})	$\alpha_2 \times 10^{-6}$ (°C^{-1})	R^2
MgF20	25–600	8.1137 (7)	8.9 (2)		0.997
	650–1000	8.1145 (15)		9.1 (5)	0.998
MgF14	25–600	8.1066 (8)	8.9 (2)		0.997
	650–1000	8.1052 (6)		9.5 (1)	1.000
3dis	25–550	8.0925 (6)	8.5 (2)		0.997
	600–1000	8.0909 (12)		9.4 (2)	0.998

Notes: Estimated standard deviation in brackets; α_1 = low-temperature range; α_2 = high-temperature range.
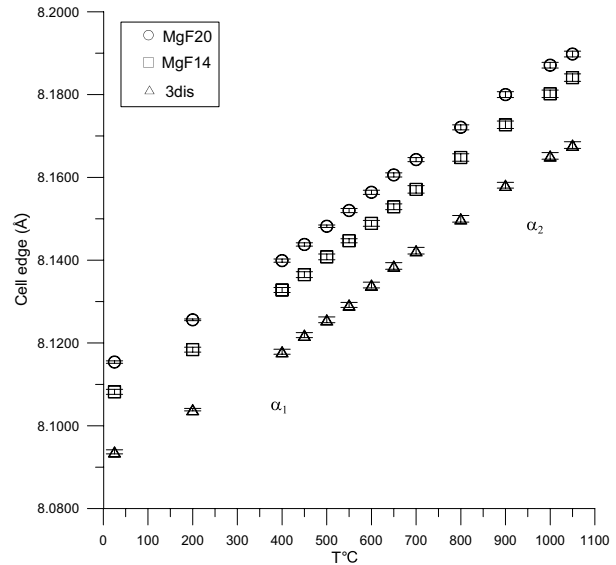

FIGURE 1. Cell edge vs. temperature relations for the three spinel samples investigated. The symbol size is as large as the estimated standard deviation. The two regressions lines, before and after the start of cation exchange, indicate slightly different α_1 and α_2 thermal expansion coefficients.

based on the O'Neill and Navrotsky (1984) thermodynamic model. As the crystals were not drop quenched after the synthesis experiments (which were carried out through slow-cooling experiments between 1200 and 900 °C), the above temperature is inevitably an overestimate of the temperature from which the observed ordering state has been effectively quenched. On the basis of the present measurements, the u values maintain ap-

proximately the same value as the untreated samples up to 650 °C, and then markedly change, revealing that cation exchanges have been effectively triggered. In fact, at 700 °C the samples were heated long enough to achieve the equilibrium state at that temperature.

For all crystals, the cation distributions obtained from experimental data collected at different temperatures are reported in Table 3. The inversion parameter i (Al + Fe^{3+} at the T site) shows the opposite slope with respect to the oxygen coordinate (cf. insets in Figs. 2a-c). For the MgF20 crystal, the i value is almost constant (ca. 0.28) from room temperature to about 550 °C, then the Fe^{3+} cation appears to reorder slightly at the M site and i reaches a minimum (0.27) at 650 °C. After this temperature and up to 1050 °C any further temperature increase is paralleled by a progressive increase of cation disorder, as illustrated by the regular rise of i values up to 0.33. Similarly, for the MgF14 crystal the inversion maintains a constant value (ca. 0.27) from room temperature to 600 °C, suddenly decreases to 0.25 at 650 °C, and then rapidly increases up to 0.32 at 1050 °C. A similar behavior, only better defined, was observed for the 3dis crystal: the inversion parameter remains constant (ca. 0.28) up to 550 °C, suddenly decreases to a minimum (0.25) at 600–650 °C, and finally increases up to 0.32 at 1050 °C. In this sample, the marked difference between the quenched-in ordering state (corresponding to ca. 800 °C) and the first equilibrium state achieved during the heating experiments (650 °C) accounts for the extensive reordering observed between 550 and 650 °C (Fig. 2c).

The observed process of cation distribution relaxation followed by disordering at the highest temperatures typically occurs when quenched material is heated slowly (cf. Redfern et al. 1999; Carbonin et al. 2002). In our samples, this is well testified by the Mg-Al exchange. In fact, starting from the ^{IV}Al quenched-in at
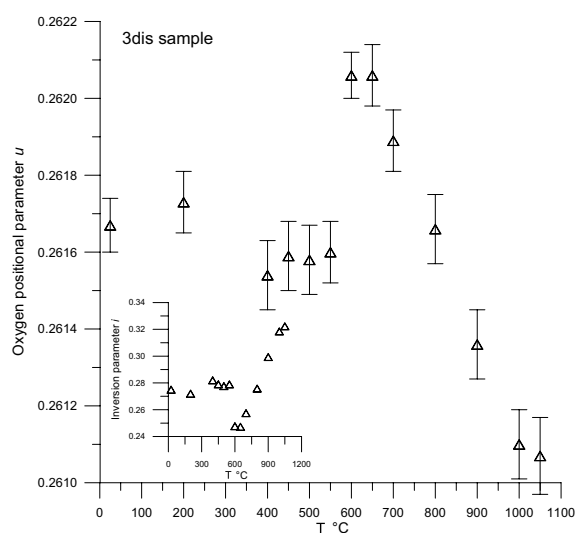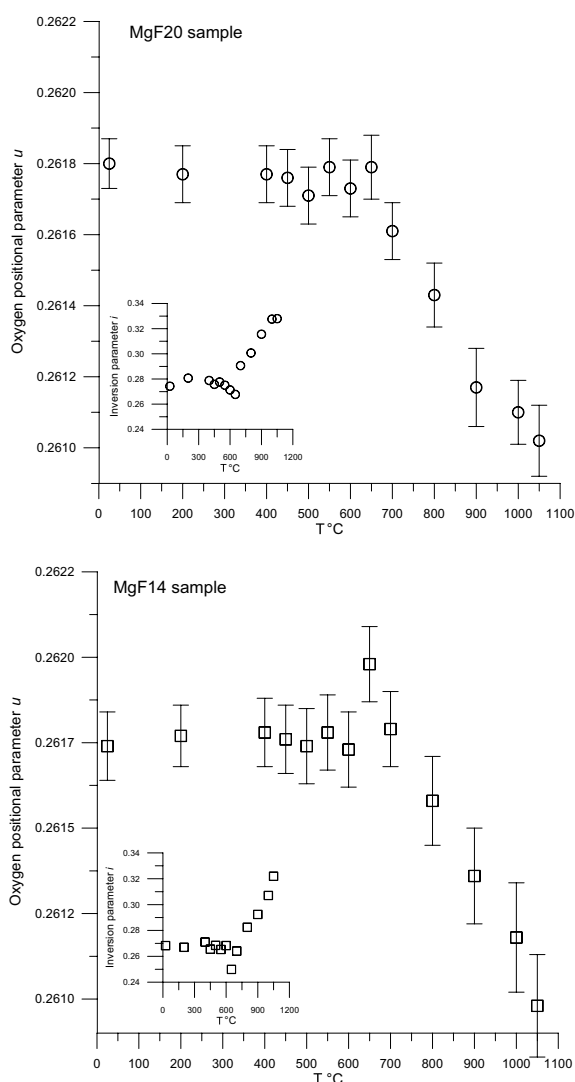
FIGURE 2. Variation of oxygen positional parameter u as a function of temperature for samples MgF20, MgF14, and 3dis. Insets: variation of experimental inversion parameter i obtained from measured cation distribution as a function of temperature (symbol sizes are of same order of magnitude as the standard deviations).

high temperature, the heating process in the range 550-650 °C determines an Al reordering at the M site, followed by progressive disordering at $T > 650$ °C. Minor evidences of cation relaxation are showed by the Mg-Fe^{3+} exchange, which could seem to be scarcely affected by temperature. However, a careful inspection of experimental data reveals that this exchange is already active around 500 °C (Table 3). Our data are in line with experimental results of Antao et al. (2005), who found onset of the Mg-Fe^{3+} exchange at about 500 °C. Moreover, Martignago et al. (2003) showed that Fe^{3+}, even in small but ordered amounts, effectively contributes to increase spinel inversion, exchanging with Mg at temperatures higher than 550 °C.

THERMODYNAMICS AND KINETICS OF MG-AL AND MG-FE^{3+} INTERSITE EXCHANGE

The temperature-dependent intracrystalline cation distribution of spinel s.s.-magnesioferrite series can be modeled by using the general thermodynamic model for spinel binary solid-solutions of O'Neill and Navrotsky (1983, 1984). By adopting its simplest formulation, cation distribution at equilibrium corresponds to the minimum free energy of disordering (ΔG_D) with respect to inversion i, i.e., $(\delta \Delta G_D /\delta i)_T = 0$. The change of enthalpy of cation disordering (ΔH_D), relative to the same spinel with normal cation distribution, was shown to vary with $\alpha_{A-B} i + \beta i^2$, where α_{A-B} is the difference in the "site preference enthalpies" of cations A and B. Combining the expression of enthalpy of mixing with the configurational entropy of a given cation distribution (ΔS_C), and considering that $\delta \Delta S_C/\delta i$ is proportional to $\ln[i^2/(1-i)(2-i)]$, the equation $-RT\ln[i^2/(1-i)(2-i)] = \alpha_{A-B} + 2\beta i$ is obtained for a single end-member.

Applying the general model to the binary solid solution Mg(Al$_{1-z}$Fe$_z^{3+}$)$_2$O$_4$, the following equations can be derived:

$$-RT\ln[x(x + y) / (1 - x - y)(2z - x)] = \alpha_{Mg\text{-}Fe3+} + 2\beta_{Mg\text{-}Fe3+}x + (\beta_{Mg\text{-}Fe3+} + \beta_{Mg\text{-}Al})y \tag{2}$$

$$-RT\ln[y(x + y) / (1 - x - y)(2 - 2z - y)] = \alpha_{Mg\text{-}Al} + 2\beta_{Mg\text{-}Al}y + (\beta_{Mg\text{-}Fe3+} + \beta_{Mg\text{-}Al})x \tag{3}$$

where $x = {}^{IV}Fe^{3+}$, $y = {}^{IV}Al$, z = magnesioferrite molar content ($2z = Fe^{3+}_{tot}$ in apfu), $\alpha_{Mg\text{-}Fe3+} = 26.6$ kJ/mol, $\beta_{Mg\text{-}Fe3+} = -21.7$ kJ/mol (O'Neill et al. 1992), and $\alpha_{Mg\text{-}Al} = 23$ kJ/mol, $\beta_{Mg\text{-}Al} = 13$ kJ/mol (Andreozzi et al. 2000). Equations 2 and 3 were solved numerically for the temperature interval 600–1100 °C and for $2z = 0.078$ (3 dis), 0.138 (MgF14), and 0.200 (MgF20). Calculated values are reported in Table 5.

The experimental inversion values compare satisfactorily with the calculated ones at temperatures higher than 650 °C, conditions under which equilibrium state was achieved at any T. Apart from a systematic overestimation of inversion, previously observed and discussed by Carbonin et al. (2002), the two

data sets closely follow the same trend (Fig. 3). In particular, the reproducibility of ^{IV}Al amounts is very high (Fig. 4), whereas the quantities of $^{IV}Fe^{3+}$ are not satisfactorily matched (Fig. 5). According to the model, $^{IV}Fe^{3+}$ should increase with both total Fe^{3+} and temperature, but experimental data seem to remain fairly constant, with just small variations in the range 450–700 °C. The percentages of $^{IV}Fe^{3+}$ with respect to Fe^{3+}_{tot} retrieved experimentally cluster around 45%, whereas the model predicts a regular increase from 13 to 24 % in the range 600–1100 °C. The overestimation of measured $^{IV}Fe^{3+}$ may be due to uncertainties in the absolute contents of Fe^{3+}_{tot}, which were too small to be accurately estimated by means of crystallographic procedures.

Our samples are essentially spinel s.s. with some 4%, 7%, and 10% magnesioferrite component. By combining experimental and thermodynamically obtained information, it follows that intersite exchanges are evidently dominated by Mg-Al exchange, yet the Mg-Fe^{3+} exchange also appears to play an important role. In fact, final inversion values at equilibrium at any T are found to be a direct function of Fe^{3+} contents (Fig. 3). Heating from 450 to 550 °C was unable to activate the Mg-Al exchange, but was able to trigger the Mg-Fe^{3+} exchange that made $^{IV}Fe^{3+}$ decrease slightly as a result of cation ordering. At about 600 °C, the Mg-Fe^{3+} distribution quickly reached equilibrium with the external temperature, and then $^{IV}Fe^{3+}$ followed a gently rising trend with T (Fig. 5). Between 550 and 650 °C, the Mg-Al exchange was activated as well, but it was not in equilibrium with the external temperature, so that ^{IV}Al decreased due to Mg-Al reordering (Fig. 4). As a result, inversion decreased down to a minimum in all the three studied samples because the amounts of Al that reordered

TABLE 5. Calculated cation distribution as a function of temperature

Sample	T (°C)	T site				M site		
		Al	Fe³⁺	Mg	i*	Al	Fe³⁺	Mg
MgF20								
	600	0.165	0.027	0.808	0.192	1.636	0.173	0.191
	700	0.188	0.032	0.780	0.220	1.613	0.168	0.219
	800	0.201	0.037	0.762	0.238	1.600	0.163	0.237
	900	0.228	0.041	0.731	0.269	1.573	0.159	0.268
	1000	0.245	0.045	0.710	0.290	1.556	0.155	0.289
	1100	0.261	0.048	0.691	0.309	1.540	0.152	0.308
MgF14								
	600	0.170	0.019	0.811	0.189	1.686	0.125	0.189
	700	0.193	0.023	0.784	0.210	1.663	0.121	0.216
	800	0.215	0.026	0.759	0.241	1.641	0.118	0.241
	900	0.235	0.029	0.736	0.264	1.621	0.115	0.264
	1000	0.253	0.032	0.715	0.285	1.603	0.112	0.285
	1100	0.269	0.034	0.697	0.303	1.587	0.110	0.303
3dis								
	600	0.175	0.010	0.815	0.185	1.748	0.067	0.185
	700	0.199	0.012	0.789	0.211	1.724	0.065	0.211
	800	0.222	0.014	0.764	0.236	1.701	0.063	0.236
	900	0.243	0.015	0.742	0.258	1.680	0.062	0.258
	1000	0.261	0.017	0.722	0.278	1.662	0.060	0.278
	1100	0.279	0.018	0.703	0.297	1.644	0.059	0.297

Notes: *i = inversion degree (Al + Fe^{3+} at the T site) calculated, see text.

FIGURE 4. Comparison among experimental and calculated ^{IV}Al variations as a function of temperature for the three studied samples. Open circles = exp. MgF20; open squares = exp. MgF14; open triangles = exp. 3dis. Bold dotted line = calc. MgF20; bold dashed line = MgF14; bold solid line = calc 3dis. Symbol sizes are the same order of magnitude as the standard deviations.
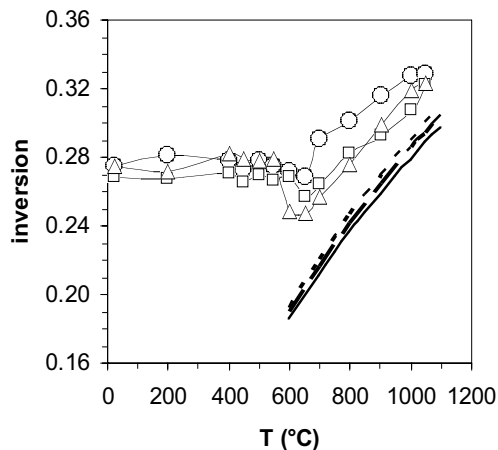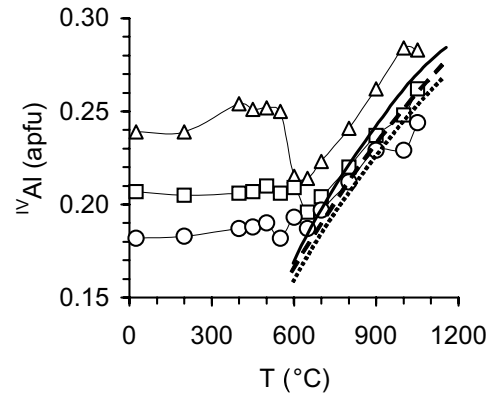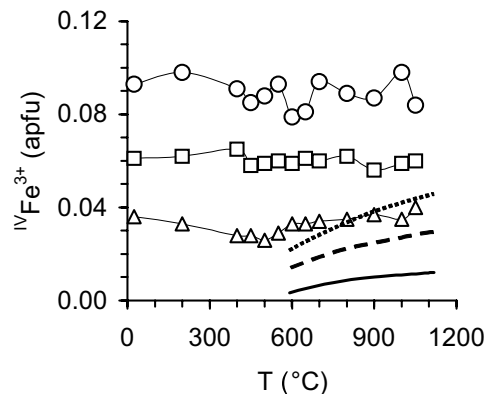

FIGURE 3. Comparison among experimental and calculated (from the model of O'Neill and Navrotsky 1983) variations of inversion parameter as a function of temperature for the three studied spinel samples. Open circles = exp. MgF20; open squares = exp. MgF14; open triangles = exp. 3dis. Bold dotted line = calc. MgF20; bold dashed line = MgF14; bold solid line = calc 3dis. Symbol sizes are the same order of magnitude as the standard deviations

FIGURE 5. Comparison among experimental and calculated $^{IV}Fe^{3+}$ variations as a function of temperature for the three studied samples. Open circles = exp. MgF20; open squares = exp. MgF14; open triangles = exp. 3dis. Bold dotted line = calc. MgF20; bold dashed line = MgF14; bold solid line = calc 3dis. Symbol sizes are the same order of magnitude as the standard deviations.

were far more abundant than those of Fe^{3+} that disordered. At about 700 °C, Mg-Al exchange achieved equilibrium with T, and then both $^{IV}Fe^{3+}$ and ^{IV}Al increased up to 1050 °C following the equilibrium path.

The temperature dependence of the kinetic constant K is expressed by the Arrhenius relation $K = A_{exp}(-E_a/RT)$. For the Mg-Al exchange, a pre-exponential factor (A) of 5.861×10^8 min^{-1} and an activation energy (E_a) of 197 ± 22 kJ/mol were obtained by Andreozzi and Princivalle (2002). On this basis, the values calculated for K at 500 and 800 °C are $K_{500} = 2.75 \ 10^{-5}$ and $K_{800} = 0.112 \ min^{-1}$. The corresponding half-life of the reaction ($t_{1/2}$), i.e., the time required to go halfway from any set of initial and final inversion degrees, is equal to 3000 h at 500 °C and 6.2 min at 800 °C. For the Mg-Fe^{3+} exchange, Harrison and Putnis (1999) obtained a pre-exponential factor of $3.978 \times 10^{11} \ min^{-1}$ and an activation energy of 217 kJ/mol. The values calculated for K at 500 and 800 °C are $K_{500} = 8.29 \times 10^{-4}$ and $K_{800} = 10.55$ min^{-1}. The corresponding $t_{1/2}$ are 14 h at 500 °C and 3.6 s at 800 °C. These data confirm that the Mg-Fe^{3+} exchange proceeds at a faster rate than the Mg-Al exchange. They also suggest that the Mg-Fe^{3+} exchange may be active at laboratory time scales down to 500 °C, as verified in the present case and previously observed by Martignago et al. (2003) and Antao et al. (2005), whereas the Mg-Al exchange may be hardly monitored below 600 °C.

As a consequence, during ordering processes, for any cooling path, Fe^{3+}-bearing alluminate spinels are expected to show final inversion values lower than Fe^{3+}-free ones, because the Mg-Fe^{3+} exchange will be quenched in at temperatures lower than the Mg-Al exchange.

REFERENCES CITED

Andreozzi, G.B. and Princivalle, F. (2002) Kinetics of cation ordering in synthetic MgAl₂O₄ spinel. American Mineralogist, 87, 838–844.
Andreozzi, G.B., Princivalle, F., Skogby, H., and Della Giusta, A. (2000) Cation ordering and structural variations with temperature in MgAl₂O₄ spinel: an X-ray single-crystal study. American Mineralogist, 85, 1164–1171.
Andreozzi, G.B., Hålenius, U., and Skogby, H. (2001) Spectroscopic active $^{IV}Fe^{3+}$ -$^{VI}Fe^{3+}$ clusters in spinel-magnesioferrite solid solution crystals: a potential monitor for ordering in oxide spinels. Physics and Chemistry of Minerals, 28, 435–444.
Antao, S.M., Hassan, I., and Parise, J.B. (2005) Cation ordering in magnesioferrite, MgFe₂O₄, to 982°C using in situ synchrotron X-ray powder diffraction. American Mineralogist, 90, 219–228.
Bothwell, D.I. and Hey, M.H. (1958) The nature of chlorospinel. Mineralogical

Magazine, 31, 885–887.
Carbonin, S., Russo, U., and Della Giusta, A. (1996) Cation distribution in some natural spinels from X-ray diffraction and Mössbauer spectroscopy. Mineral-ogical Magazine, 60, 355–368.
Carbonin, S., Martignago, F., Menegazzo, G., and Dal Negro, A. (2002) X-ray single-crystal study of spinels: in situ heating. Physics and Chemistry of Minerals, 29, 503–514.
Della Giusta, A., Princivalle, F., and Carbonin, S. (1986) Crystal chemistry of a suite of natural Cr-bearing spinels with 0.15≤Cr≤1.07. Neues Jahrbuch für Mineralogie Abhandlungen, 155, 319–330.
Ganguly, J. (1982) Mg-Fe order-disorder in ferromagnesian silicates. II. Thermo-dynamics, kinetics, and geological applications. In S.K. Saxena, Ed., Advances in Physical Geochemistry, 2, 58–99. Springer, New York.
Harrison, R.J. and Putnis, A. (1999) Determination of the mechanism of cation ordering in magnesioferrite (MgFe₂O₄) from the time- and temperature-de-pendence of magnetic susceptibility. Physics and Chemistry of Minerals, 26, 322–332.
Harrison, R.J., Redfern, S.A.T., and O'Neill, H.St.C. (1998) The temperature de-pendence of the cation distribution in synthetic hercynite (FeAl₂O₄) from in situ neutron diffraction refinements. American Mineralogist, 83, 1092–1099.
Lavina, B., Salviulo, G., and Della Giusta, A. (2002) Cation distribution and structure modelling of spinel solid solutions. Physics and Chemistry of Minerals, 29, 10–18.
Martignago, F., Dal Negro, A., and Carbonin, S. (2003) How Cr^{3+} and Fe^{3+} affect Mg-Al order disorder transformation at high temperature in natural spinels. Physics and Chemistry of Minerals, 30, 401–408.
Molin, G., Martignago, F., and Dal Negro, A. (2001) A new radiative microfurnace for X-ray single-crystal diffractometry. European Journal of Mineralogy, 13, 557–563.
Mueller, R.F. (1967) Model for order-disorder kinetics in certain quasi-binary crystals of continuously variable composition. Journal of Physics and Chemistry of solids, 28, 2239–2243.
——— (1969) Kinetics and thermodynamics of intracrystalline distribution. Mineralogical Society of America Special Paper, 2, 83–93.
O'Neill, H.St.C. (1994) Kinetics of cation order-disorder in MgFe₂O₄ spinel. European Science Foundation Program on Kinetic Processes in Minerals and Ceramics, Proceedings of the Workshop on Kinetics of Cation Ordering, Cambridge, England.
O'Neill, H.St.C. and Dollase, W.A. (1994) Crystal structures and cation distribution in simple spinels from powder XRD structural refinements: MgCr₂O₄, ZnCr₂O₄, Fe₃O₄ and the temperature dependence of the cation distribution in ZnAl₂O₄. Physics and Chemistry of Minerals, 20, 541–555.
O'Neill, H.St.C. and Navrotsky, A. (1983) Simple spinels: crystallographic parameters, cation rdii, lattice energies, and cation distribution. American Mineralogist, 68, 181–194.
——— (1984) Cation distribution and thermodynamic properties of binary spinel solid solution. American Mineralogist, 69, 733–753.
O'Neill, H.St.C., Annersten, H., and Virgo, D. (1992) The temperature dependence of the cation distribution in magnesioferrite (MgFe₂O₄) from powder XRD structural refinements and Mössbauer spectroscopy. American Mineralogist, 77, 725–740.
Redfern, S.A.T., Harrison, R.J., O'Neill, H.St.C., and Wood, D.R.R. (1999) Thermodynamics and kinetics of cation ordering in MgAl₂O₄ spinel up to 1600 °C from in situ neutron diffraction. American Mineralogist, 84, 299–310.
Salviulo, G., Carbonin, S., and Della Giusta, A. (2000) Powder and single-crystal X-ray structural refinements on a natural chromite: dependence of site occupancies on experimental strategies. Materials Science Forum, 321–324, 46–52.
Sheldrick, G.M. (1997) SHELXL-97, a program for crystal structure refinement. University of Göttingen, Germany.